JES Focus Issue on Electrocatalysis — In Honor of Radoslav Adzic

Potential-Dependent Adsorption of CO and Its Low-Overpotential Reduction to CH_3CH_2OH on Cu(511) Surface Reconstructed from Cu(pc): Operando Studies by Seriatim STM-EQCN-DEMS

Chu F. Tsang,[1,2] Alnald C. Javier,[1] Youn-Geun Kim,[1,*] Jack H. Baricuatro,[1] Kyle D. Cummins,[1] Jutae Kim,[3] Gregory Jerkiewicz,[3] John C. Hemminger,[2] and Manuel P. Soriaga [1,z]

[1] *Joint Center for Artificial Photosynthesis, California Institute of Technology, Pasadena, California 91125, USA*
[2] *Department of Chemistry, University of California, Irvine, Irvine, California 92697, USA*
[3] *Department of Chemistry, Queen's University, Ontario K7L 3N6, Canada*

Operando scanning tunneling microscopy first revealed that application of a CO_2-reduction potential to a Cu(pc) electrode in 0.1 M KOH resulted in the reconstruction of the selvedge to an x-layer stack of well-ordered Cu(100) terraces, Cu(pc)-x[Cu(100)]. Subsequent Cu↔Cu_2O oxidation-reduction cycles between −0.90 V and 0.10 V SHE converted the reconstructed region to a stepped Cu(S)-[3(100) × (111)], or Cu(511), surface. Differential electrochemical mass spectrometry showed that reduction of CO produced only CH_3CH_2OH at the lowest overpotential. Later application of STM and surface infrared spectroscopy uncovered a potential, above which no CO adsorption occurs. In this study, electrochemical quartz crystal nanobalance was combined with STM and DEMS as a prelude to the acquisition of CO coverages as continuous functions of concentration and potential; in heterogeneous catalysis, surface coverage are important since the reaction rate are functions of those quantities. Also equally critical is the knowledge of the packing arrangement at the onset of the reaction because, if "CO dimers" were indeed the precursors to C_{2+} products, reduction can only be initiated when the adlayer consists of closely packed CO; otherwise, dimerization will not transpire if the molecules were far apart. The results indicate that the catalysis lags the adsorption, and starts only when CO adsorption is saturated.

 [DOI: 10.1149/2.0451815jes]

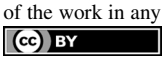

Manuscript submitted August 10, 2018; revised manuscript received October 15, 2018. Published November 15, 2018. *This paper is part of the JES Focus Issue on Electrocatalysis — In Honor of Radoslav Adzic.*

Seriatim or sequential operando scanning tunneling microcopy (STM) and polarization-modulation infrared spectroscopy (PMIRS) were recently applied to determine the adsorption of carbon monoxide on Cu(100) at preselected potentials, −0.90 V, −0.85 V, and −0.80 V (SHE), in 0.1 M KOH bubble-saturated with CO.[1] At the latter potential, no CO adsorption took place; at −0.85 V and −0.90 V, CO was adsorbed to form a Cu(100)-c(2 × 2)-CO adlattice structure of fractional coverage θ_{CO}[a] equal to 0.5. The vibrational-frequency shift ($\Delta\nu \approx 118\ cm^{-1}$) of the C≡O stretch mode relative to that of unbound CO indicated weak vertical adsorption on a one-fold (atop) site, consistent with results extracted from dynamical low-energy electron diffraction (LEED) of CO on Cu(100) in ultrahigh vacuum at 80 K,[3] and with the absence of evidence for non-vertically-adsorbed CO in the STM images. The adsorptive properties of CO on Cu is important because, as is well-known for heterogeneous catalytic processes, the rate of the reaction is dependent upon the surface coverage of the starting material: no adsorption, no surface-catalyzed reaction. Additionally, a "CO dimer" has been postulated as the precursor-intermediate in the formation of pure and oxygenated C_{2+} hydrocarbons.[4,5] No evidence for adsorbed dimers were found in our *seriatim* STM-PMIRS work, most likely because the adsorbed intermediates are short-lived, and our experiments were not time-resolved. Nevertheless, given the results under static conditions, the computer-simulated mechanistic flow needs to take into account not only the less-than-optimal CO_{ads}-CO_{ads} distance, but also the distortion of the linearly-and-singly adsorbed CO molecules to enable side-by-side, side-to-end, or end-to-end dimerization.

In the present work, an adjunct to the previous operando studies, electrochemical quartz-crystal nanobalance (EQCN) was employed with a stepped Cu(S)-[3(100) × (111)], or Cu(511), surface, formed from the potential-induced surface reconstruction of a pre-oxidized, or nominally oxide-derived,[6] polycrystalline Cu disk electrode,[7,8] to obtain an extended θ_{CO}-vs-E plot in the range from −0.65 V to −0.95 V. The merit of this graph unfolds when it is juxtaposed with the potential-dependence of the CO-to-CH_3CH_2OH reduction, as represented by the DEMS ethanol-ion-current-vs-E data; it may be recalled that, on Cu(511)[8] and at oxide-derived polycrystalline Cu nanoparticles,[6] the reduction of CO to ethanol in 0.1 M KOH, occurs at the lowest overpotential observed, ca. 645 mV less than what generates multiple products.[7] The comparison is expected to show that the onset potential for the reduction reaction would occur later than that for the adsorption process; if the catalytic reduction starts only after a (nearly) space-filling CO adlayer is completed, it may indirectly suggest that "CO dimers" are indeed involved in the production of ethanol; such dimers would almost certainly not be formed in, for example, a quarter-coverage CO adlayer, $\theta_{CO} = 0.25$.

Experimental

Electrochemical STM.—Detailed aspects of operando STM have been discussed previously.[1,7,8] A refurbished (Advanced Surface Microscopy, Inc., Indianapolis, IN) Nanoscope E microscope (Digital Instruments, Santa Barbara, CA), interfaced with a three-electrode potentiostat, was employed. STM probes were fabricated from small-diameter tungsten wires (Millipore Sigma, St. Louis, MO) etched to sharpness at 15 VAC in 0.6 M KOH. STM images in 0.010 M KOH solution were acquired with a high-resolution scanner employed in constant-current mode without post-scan operations. The reference electrode was Ag/AgCl (3.4 M KCl) in a miniature, leakless cell; the counter electrode was a Pt wire. The potentials reported here are with respect to SHE based on the conversion: E Ag/AgCl (3.5 M KCl) = 0.205 V SHE.[9] The measured resistance of the ECSTM cell was 30 Ω at a prevailing current of ca. −12.0 μA at −0.90 V (SHE). The resultant IR-drop is ca. 0.36 mV, a negligible correction to the potential at which the ECSTM images was acquired. High-purity (95%) carbon monoxide was purchased from Airgas (Welding Supply Store, Duarte, CA). The 0.10 M KOH electrolytic solution was prepared from Barnstead NANOpure water (18.2 MΩ-cm) and analytical-grade KOH

*Electrochemical Society Member.
[z]E-mail: msoriaga@caltech.edu

[a]θ is defined here as $\Gamma_{adsorbate}/\Gamma_{substrate}$, where $\Gamma_{adsorbate}$ is the surface concentration (mol cm^{-2}) of the adsorbate, and $\Gamma_{substrate}$ is that for the substrate surface atoms; the latter will depend upon the particular surface crystallographic orientation.[2]

(Millipore Sigma, St. Louis, MO). All experiments were carried out at 298 K.

Preparation of Cu(511) for DEMS.—Differential electrochemical mass spectrometry has been described elsewhere,[10] and only aspects related to the preparation of the Cu(511), surface are outlined here. A 99.99%-pure polycrystalline Cu disk (Goodfellow, Coraopolis, PA), 1.0 cm in diameter and 0.15 mm in thickness, was metallographically polished and electropolished for 10 s in 85% phosphoric acid solution (Sigma-Aldrich, St. Louis, MO) at 2.1 V against a 99.8%-pure graphite rod (Alfa Aesar, Ward Hill, MA). After a thorough rinse in Nanopure water, a potential of −0.9 V (vs. SHE) was applied to the Cu electrode in a N_2-saturated 0.1 *M* KOH solution (Sigma-Aldrich) for 2 hours to convert the initially disordered polycrystalline surface to well-ordered Cu(100) single-crystal layers. This was followed by multiple monolayer-limited oxidation-reduction cycles (ORC) between 0.1 V and −0.9 V to induce surface reconstruction from Cu(pc)-[Cu(100)] to Cu(pc)-[Cu(511)].[7] With a protective layer of 0.1 M KOH electrolyte, the Cu(511) electrode was then placed inside the DEMS cell pre-filled with a CO-bubble-saturated solution of 0.1 M KOH. The potential was held for 600 s each at preselected values of −1.07 V, −1.02 V, −0.97 V, −0.92 V, −0.77 V and −0.67 V, as the ion current for m/z = 31 (ethanol) was monitored by an HPR-20 quadrupole mass spectrometer (Hiden Analytical, Warrington, England) equipped with a secondary electron multiplier detector set at a voltage of 950 V and an emission current of 500 μA. The ethanol MS signals at 600 s were plotted as a function of applied potential. The base peak of ethanol at m/z = 31 is shared by methanol but the correct peak assignment is ensured by the congruence of the ratio of the analytical signals at m/z = 31 and 45 to the signal ratio generated by an ethanol standard.[7] In the established absence of methanol, the signal at m/z = 31, due to its favorably high signal-to-noise ratio, was used to track ethanol production.

EQCN.—A quartz crystal nanobalance (QCN) was used to measure, under electrochemical reaction conditions, the changes in the frequency, Δf, of a quartz resonator when variations in mass (Δm) transpire at the surface.[11,12] The EQCN data were acquired with a Seiko-EG&G QCA922 analyzer (Bio-logic, Knoxville, TN) interfaced to a Bio-Logic SP-200 potentiostat. The EQCN cell, reminiscent of classic H-cells, was constructed from Pyrex glass, Figure 1, based on a design by the Jerkiewicz group at Queen's University.[13] The bottom part of the main compartment held the resonator, doubled as the working electrode, in a horizontal configuration. A gold wire served as the auxiliary electrode. The reference electrode, located in the outer compartment, was a reversible hydrogen electrode (RHE) brought in close proximity to the working electrode by a Luggin capillary. Potentiostatic electrochemical impedance was performed at 100 kHz to determine the uncompensated solution resistance, R_u; 85% of R_u was electronically compensated, akin to the corrections made to the DEMS results.[10]

The resonator-electrode was an AT-cut quartz crystal with 9-MHz resonance frequency, coated on both sides with ca. 300 nm-thick Cu; it was mounted onto a PTFE holder so that only one side would be in contact with the solution. The EQCN cell was set on a platform suspended by bungee cords inside a custom-built Faraday enclosure that insulated against electromagnetic fields. The entire cage was itself mounted on a solid-rubber stage for vibration isolation. The pretreatment of the Cu film electrode prior to the EQCN measurements were as described above, but potentiostatic (e.g., CO preadsorption at −1.06 V) and cyclic voltammetric (CV) operations (e.g., between 0.1 V to −0.9 V) were such that the Cu(pc) surface would have been reconstructed to Cu(511), as later confirmed by an ethanol-product-only DEMS result. The electrochemical surface area (ECSA) of the Cu electrode was determined by monolayer-limited underpotential deposition (UPD) of Pb, a process previously described in the literature.[14] The use of Cu_2O-formation to assay the ECSA did not prove keenly reliable because the oxidation peak is broad and includes a small but indeterminable amount of CuO. Application of Faraday's Law on the Pb UPD charge, and in consideration of the difference in the atomic radii of Cu (145 pm) and Pb (154 pm), yielded a value of 0.30 cm^2 for the Cu ECSA; this corresponded to a surface roughness of ca. 1.5, typical of that for Pt-coated resonators processed similarly.[15]

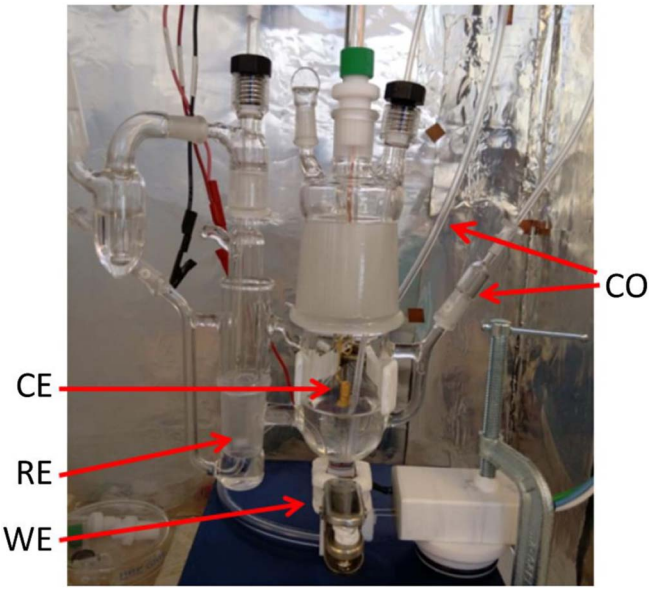

Figure 1. Picture of the electrochemical quartz-crystal nanobalance. One of the CO ports is for direct sparging of CO into the solution, the other is for CO circulation in the head space. CE: Pt counter electrode. RE: SHE reference electrode. WE: Cu-film electrode on quartz crystal resonator.

For the EQCN CO-adsorption measurements, the Cu electrode was first held under N_2 purge for at least 60 s at −1.06 V, the potential at which CO would be pre-adsorbed at the maximum coverage.[1] The N_2 was then replaced by CO and an adsorption time of 30 s was allowed; no differences were found at longer exposure times. Unfortunately, when unadsorbed CO was present in the solution, the noise level of the total frequency transient increased markedly, and that resulted in the obstruction of the lower-noise-level Δf attributable only to the CO adsorption. To circumvent this complication, unadsorbed CO had to be purged by N_2 from both solution and head space prior to the frequency-transient measurements. Control or blank experiments were carried out identically but with N_2 gas only. In typical EQCN experiments Δm is extracted from Δf via the Sauerbrey equation.[11] In this work, however, the EQCN data were directly converted to θ_{CO}, by calibration with PMIRS data on Cu(pc)-[Cu(511)]. For example, θ_{CO} at −0.9 V and at E ≥ −0.8 V were found to be 0.50 and 0.0, respectively; consequently, the EQCN coverage data at these potentials were made equivalent to the STM-PMIRS values. In this context, it will be mentioned that non-PM IRS data for CO chemisorbed on pristine Pt(100) and Pt(511) single crystals showed essentially identical coverages.[16]

Results and Discussion

The formation of surface-reconstructed interfacial layers of Cu(100) and Cu(511) from polycrystalline Cu(pc) anodically oxidized at 0.1 V in CO-free 0.1 M KOH is illustrated in the step-scan operando STM images[b] in Figure 2.[7] Inset A shows a 200 nm × 200 nm ECSTM image of the Cu(pc) electrode after a 30-s reduction at −0.9 V; the existence of a disordered, still oxidized, surface is evident. Inset B shows the same surface after 60 m at −0.9 V; at

[b]While it may seem that the STM images depict only nanometer-scale domains on the bulk crystal, those are actually representative of the entire surface based upon a comparison with numerous images from randomly selected areas. The default protocol in STM work has always been that images will be published only if satisfactory agreement exists among all the sampled images.

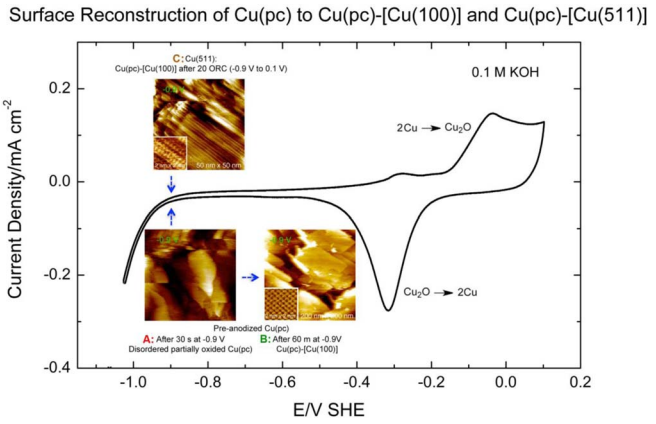

Figure 2. Combined cyclic voltammetry and scanning tunneling microscopy that illustrate the preparation of the stepped Cu(511) surface via the potentiostatic surface reconstruction of Cu(pc) at E < −0.9 V in 0.1 M KOH, followed by oxidation-reduction cycles between −0.9 V and 0.1 V. The geometric area of the single crystal was 1.0 cm^2. The potential sweep rate was 50 mV s^{-1}. Experimental parameters: Bias voltage = −300 mV. Tunneling current: low-resolution images: 2 nA; high-resolution images: 5 nA.

this stage, surface reconstruction has already resulted in well-ordered wide terraces of (100) orientation. When the latter surface is subjected to multiple ORC between 0.1 V and −0.9 V, further reconstruction ensues to yield a stepped surface, Cu(S)-[3(100) × (111)], or Cu(511). It will be noted that, at potentials more positive than −0.7 V, disordered surface Cu_2O starts to form that prevents the observation of atomic-level images; but it is remarkable that, when the potential is returned to −0.9 V, the well-ordered, oxide-free Cu(100) or Cu(511) structures are immediately restored. It is not known accurately at this time how many of the reconstructed monocrystalline layers are formed.

Figure 3 overlays a triad of DEMS plots from various Cu surfaces during the electrocatalytic reduction of CO in 0.1 M KOH. Evidently, only the electrochemically generated Cu(511), in red trace, produces ethanol at −1.06 V (SHE). CH_3CH_2OH and other reduced products

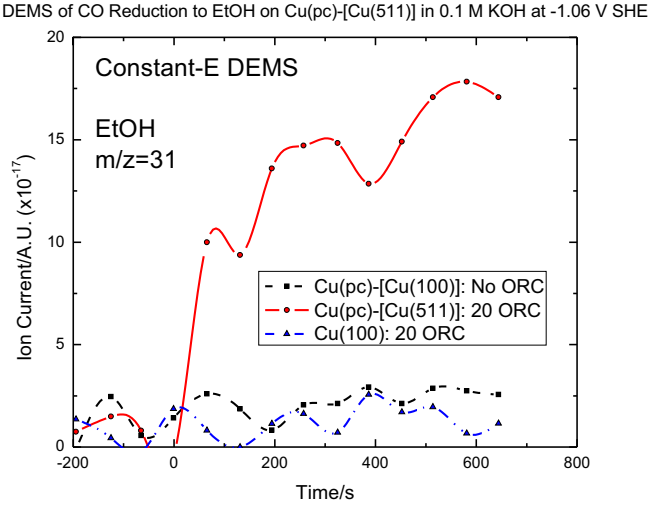

Figure 3. Differential electrochemical mass spectrometry of a 0.1 M KOH solution saturated with CO at −1.06 V SHE. Black: Reconstructed Cu(pc)-[Cu(100)] without prior oxidation-reduction cycles. Blue: Pristine Cu(100) bulk single-crystal after twenty oxidation-reduction cycles (ORC). Red: Reconstructed Cu(pc)-[Cu(511)] after multiple ORC from −0.9 V to 0.1 V. The lines do not imply any theoretical fit but serve as visual guides. The DEMS signals shown were only for m/z = 31, the base peak for CH_3CH_2OH. The fragment ratio for m/z = 31 and m/z = 45 corresponded to that of a CH_3CH_2OH standard, but the ion-current plots for m/z = 45 are not reported here.

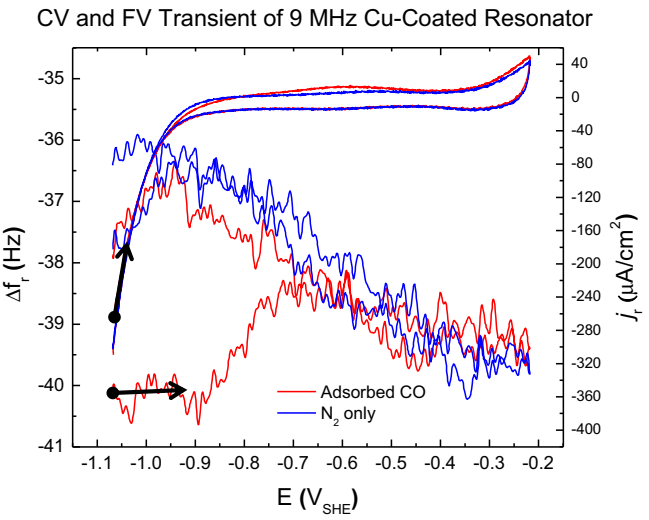

Figure 4. Cyclic voltammograms (CV) and frequency variation Δf_r (FV) transients of Cu-coated resonator in 0.1 M KOH, with (red trace) and without (blue trace) CO preadsorption at −1.06 V, followed by bubbling the electrolyte and purging the headspace with N_2 under the same potential-hold. The black arrows indicate the initial direction of the scan. The difference between the Δf_r transients in the upper and lower red trace was used to extract the CO coverage at a given potential from Equation 1 as described in the text. Potential scan rate: 20 mV s^{-1}.

such as ethylene, C_2H_4, and methane, CH_4, are produced on Cu surfaces at onset potentials ca. 150 mV more negative[7,8] than the potential applied in the present experiment. The overpotential reported here for CH_3CH_2OH production on Cu(511) is by far the lowest among the other hydrocarbon and oxygenated products formed on Cu(pc). The results in Figures 2 and 3 represent an unprecedented correlation, under actual reaction conditions, between surface structure and product selectivity.

Unlike on pristine Cu(100) surfaces, distinct atomic-level STM images could not be obtained on Cu(511) when CO is adsorbed. But that cannot be taken to signify the absence of adsorbed CO since, as described in the previous paragraph, both the DEMS and PMIRS data, and, in the same vein, the IRS experiments of CO on Pt(100) and Pt(511),[16] indicate otherwise. The possibilities exist that: (i) because of the low-overpotential activity at Cu(511), the initial reduction, regardless of how minute, already renders the images indistinct, an effect analogous to what is observed even before the actual onset of bulk Cu_2O formation;[7,8] or, (ii) the limited (3-atom) width of the Cu(100) terraces, hemmed in by the likely more reactive Cu(111) step-edges, mitigates the formation of stable well-ordered sub-nanometer structures.

The current-potential curve for Cu(511) in 0.1 M KOH is shown in Figure 4 along with the total-frequency-variation transients Δf-vs-E when CO is preadsorbed on the surface (at −1.06 V), and when only N_2 is present in solution; it is clear from the CV that, at E > −0.4 V, the $Cu \leftrightarrow Cu_2O$ reaction becomes predominant. It should first be noted that, while the frequency-transient plot for N_2 shows no hysteresis, that for CO can only be started from −1.06 V and initially traversed in the positive direction. Given the Sauerbrey equation, $\Delta f = -C_f(\frac{\Delta m}{A})$,[11] where Δm is the mass change, A the piezoelectric area, and C_f the frequency-to-mass conversion factor, it can be inferred that the decrease in Δf (i.e., the increase in Δm) at E > −0.7 V for N_2 is due to the formation of Cu_2O; for CO, the weight increase is the net change given the desorption of CO and the creation of Cu_2O. The irreversibility of the CO frequency-transient plot is a result of the fact that the desorbed CO becomes unrecoverable: When a nmol of CO, the quantity initially adsorbed on 1 cm^2 of Cu, is released to 50 mL of solution, the volume of the EQCN cell, a concentration of 20 nM is produced, too minute to rekindle adsorption.

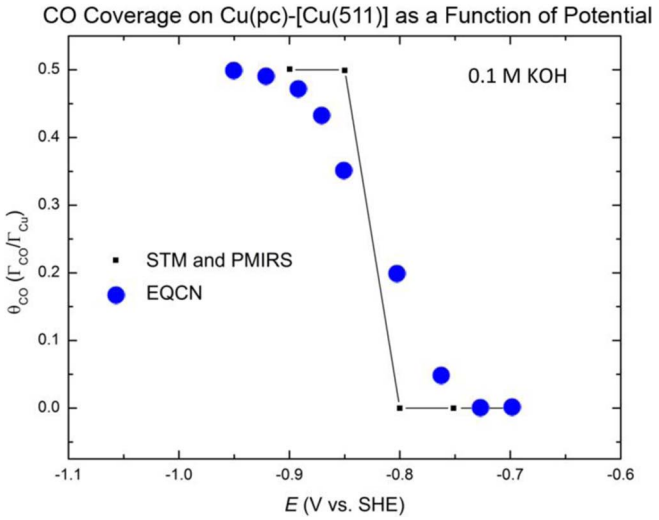

Figure 5. Adsorbed-CO coverage on Cu(511) as a function of potential in 0.1 M KOH. The square points are composite data from the STM images and the polarization-modulation infrared absorption spectra. The blue circles are based on the EQCN data. The sizes of the data points represent the comparative uncertainties in the θ_{CO} values. The solid line simply interconnects the data points and does not imply any theoretical fit.

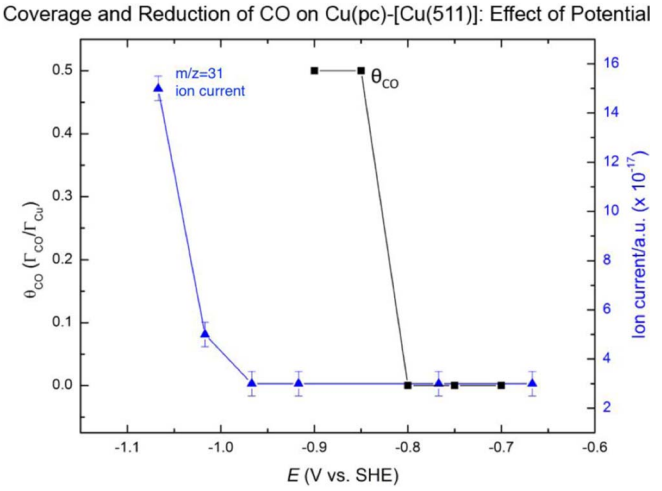

Figure 6. Plots of θ_{CO} and mass spectrometric ion currents for the formation of CH_3CH_2OH as functions of electrode potential in 0.1 M KOH. The individual points are acquired from discrete potentiostatic, rather than potentiodynamic, experiments. The solid lines simply connect the data points and do not imply any theoretical fit.

The adsorbed-CO Δf-vs-E plot (red trace) in Figure 4 that starts at -1.06 V, when the CO coverage is at maximum, and ends at -0.2 V, when the surface is entirely Cu_2O, represents a potentiometric CO-desorption scan. Since no readsorption transpires on a return sweep, the difference between the Δf of the positive (p) and negative (n) scans, at the same potential E_i, can then be taken as the adsorbed-CO-only frequency transient at that voltage:

$$\Delta f_{CO}(E_i) = \Delta f_p(E_i) - \Delta f_n(E_i) \quad [1]$$

As already stipulated above, the conversion of the frequency transient Δf_{CO} to surface coverage θ_{CO} did not rely on a Sauerbrey-equation calibration but by reference to the combined STM-PMIRS data[1c]. Hence, at -1.06 V, or -0.9 V, Δf_{CO} was set to $\theta_{CO} = 0.5$; the rest of the coverages based on this standard are given in Figure 5. Also shown in the Figure are the five STM-PMIRS data points, values that enjoy higher precision than the EQCN measurements. It is important to point out that the EQCN θ_{CO} values should have all been zero at $E > -0.8$ V; however, the noise level in the transients are such that a true zero for Δf_{CO}, obvious from a visual inspection in Figure 4, could not be obtained digitally. The comparatively low reliability of the Δf_{CO} data is the reason the EQCN-based and STM-PMIRS values were not averaged.

A comparison of the potential dependencies of the CO surface coverage and the ethanol-selective catalytic activity of Cu(511) can be gleaned from Figure 6 in which the θ_{CO}-vs-E isotherm is juxtaposed with the ethanol ion-current DEMS spectrum. Two major differences are obvious but need to be emphasized: (i) the adsorption of CO occurs much sooner, by approximately 150 mV, than the onset of the CO-to-CH_3CH_2OH reaction; and (ii) the reduction of CO does not begin until the maximum coverage of adsorbed CO is attained. The lag in the catalytic reaction, relative to the adsorption process, is not an uncommon outcome because the catalysis is heterogeneous and there would be no reaction without prior adsorption. However, it is not a requirement that the catalysis start only after full coverage is attained; the reaction could very well begin much earlier. But the latter result may lend indirect support to the postulate that "CO dimers" are intermediates in and precursors to the formation of ethanol, a C_2 product. In such an event, it would not be illogical to invoke the necessity of saturation coverage since that is the only situation in which the surface-coordinated, vertically oriented CO molecules would be closest to one another, at $d_{CO\text{-}CO} = 0.36$ nm.

At $E < -0.85$ V, θ_{CO} ($\equiv \Gamma_{CO}/\Gamma_{CO,Sat}$) becomes fixed at 0.5; no additional chemisorption takes place since all available surface-coordination (adsorption) sites have already been taken up. At $E \approx -0.975$ V, the reductive desorption of the product ethanol is initiated. At this (and at more negative) potential, however, the aqueous CO becomes much more susceptible toward adsorption; consequently, any surface site vacated by an outgoing ethanol would be immediately occupied by CO. As a result, θ_{CO} remains constant at 0.5.

It is not possible to extract correct kinetic parameters from the limited data of the present study. Nevertheless, it may be qualitatively, but confidently, conjectured from the results that, in the mechanistic progression of (i) reactant adsorption, (ii) multi-step surface reactions, and (iii) product desorption, the rate-determining step lies within the second stage such as, perhaps, the postulated formation of a "CO dimer".

Summary

Operando electrochemical quartz-crystal nanobalance was combined with scanning tunneling microscopy and differential electrochemical mass spectrometry to investigate the potential-dependencies of the adsorption of CO and its low-overpotential selective reduction to CH_3CH_2OH at a stepped Cu(511) surface; the latter was prepared from the potentiostatic surface reconstruction of Cu(pc) at $E < -0.9$ V in 0.1 M KOH, followed by monolayer-limited oxidation-reduction cycles between -0.9 V and 0.1 V. The results indicate that the electrocatalytic reduction lags the adsorption process and, in fact, does not start until maximum CO adsorption is attained. The latter may indirectly suggest that the formation of "CO dimers" is involved in the production of ethanol, since such dimers would most likely not be formed if the CO coverage (θ_{CO}) in the adsorbed layer is much lower than 0.5; that is, the distance between the CO admolecules would be too large to effect dimerization.

Acknowledgment

This material is based upon work performed by the Joint Center for Artificial Photosynthesis, a DOE Energy Innovation Hub, supported

[c]We have not actually employed PMIRS data alone to obtain an adsorption coverage (Γ or θ) because the conversion of PMIRS peak intensities to coverage would require prior calibration, but no accurate value of Γ under operando conditions is available a priori. The PMIRS peaks reveal only the presence, but not the quantity, of adsorbed CO. The present study has instead relied more on the ECSTM data to extract the Γ values.

through the Office of Science of the U. S. Department of Energy under Award No. DE-SC0004993.

ORCID

Manuel P. Soriaga https://orcid.org/0000-0002-0077-6226

References

1. J. H. Baricuatro, Y.-G. Kim, C. L. Korzeniewski, and M. P. Soriaga, "Seriatim ECSTM-ECPMIRS of the adsorption of carbon monoxide on Cu(100) in alkaline solution at CO_2-reduction potentials," *Electrochem. Commun.*, **91**, 1 (2018).
2. G. A. Somorjai, *Introduction to Surface Chemistry and Catalysis*, p. 302, John Wiley & Sons, New York (1994).
3. S. Andersson, "Vibrational excitations and structure of CO chemisorbed on Cu(100)," *Surf. Sci.*, **89**, 477 (1979).
4. M. Gattrell, N. Gupta, and A. Co, "A review of the aqueous electrochemical reduction of CO_2 to hydrocarbons at copper," *J. Electroanal. Chem.*, **594**, 1 (2006).
5. K. J. P. Schouten, Y. Kwon, C. J. M. Van der Ham, Z. Qin, and M. T. M. Koper, "A new mechanism for the selectivity to C_1 and C_2 species in the electrochemical reduction of carbon dioxide on copper electrodes," *Chem. Sci.*, **2**, 1902 (2011).
6. C. W. Li, J. Ciston, and M. W. Kanan, "Electroreduction of carbon monoxide to liquid fuel on oxide-derived nanocrystalline copper," *Nature*, **508**, 504 (2014).
7. Y.-G. Kim, A. Javier, J. H. Baricuatro, and M. P. Soriaga, "Regulating the product distribution of CO reduction by the atomic-level structural modification of the Cu electrode surface," *Electrocatalysis*, **7**, 1 (2016).
8. Y.-G. Kim A. Javier, J. H. Baricuatro, D. Torelli, K. D. Cummins, C. F. Tsang, J. C. Hemminger, and M. P. Soriaga, "Surface reconstruction of pure-Cu single-crystal electrodes under CO-reduction potentials in alkaline solutions: A study by seriatim ECSTM-DEMS," *J. Electroanal. Chem.*, **780**, 290 (2016).
9. A. Javier, J. H. Baricuatro, Y.-G. Kim, and M. P. Soriaga, "Overlayer Au-on-W near-surface alloy for the selective electrochemical reduction of CO_2 to methanol: empirical (DEMS) corroboration of a computational (DFT) prediction," *Electrocatalysis*, **6**, 493 (2015).
10. A. Javier, B. Chmielowiec, J. Sanabria-Chinchilla, Y.-G. Kim, J. H. Baricuatro, and M. P. Soriaga, "A DEMS study of the reduction of CO_2, CO, and HCHO pre-adsorbed on Cu electrodes: empirical inferences on the CO_2RR mechanism," *Electrocatalysis*, **6**, 127 (2015).
11. T. Nomura and M. Iijima, "Electrolytic determination of nanomolar concentrations of silver in solution with a piezoelectric quartz crystal," *Anal. Chim. Acta*, **131**, 97, (1981).
12. S. Bruckenstein and M. Shay, "An in situ weighing study of the mechanism for the formation of the adsorbed oxygen monolayer at a gold electrode," *J. Electroanal. Chem.*, **188**, 131, (1985).
13. G. Jerkiewicz, G. Vatankhah, A. Zolfaghari, and J. Lessard, "Analysis of the mass response of the electrochemical quartz-crystal nanobalance in horizontal and vertical geometry," *Electrochem. Commun.*, **1**, 419 (1999).
14. T. P. Moffat, "Oxidative chloride adsorption and lead upd on Cu(100): investigations into surfactant-assisted epitaxial growth," *J. Phys. Chem. B*, **102**, 10020 (1998).
15. G. Vatankhah, J. Lessard, G. Jerkiewicz, A. Zolfaghari, and B. E. Conway, "Dependence of the reliability of electrochemical quartz-crystal nanobalance mass responses on the calibration constant, C_f: analysis of three procedures for its determination," *Electrochim. Acta*, **48**, 1613 (2003).
16. R. M. Arán-Ais, M. C. Figueiredo, F. J. Vidal-Iglesias, V. Climent, E. Herrero, and J. M. Feliu, "On the behavior of the Pt(100) and vicinal surfaces in alkaline media," *Electrochim. Acta*, **58**, 184 (2011).